PREDICTION OF THE LOCAL AIR EXCHANGE RATE IN ANIMAL OCCUPIED ZONES OF A NATURALLY VENTILATED BARN

Moustapha Doumbia[1], Sabrina Hempel[1], David Janke[1] and Thomas Amon[1,2]

[1]Leibniz Institute for Agricultural Engineering and Bioeconomy, Department of Engineering for Livestock Management, Potsdam, Germany

[2]Institut of Animal Hygiene and Environmental Health, Department of Veterinary Medicine, Freie Universität Berlin, Germany

mdoumbia@atb-potsdam.de, SHempel@atb-potsdam.de, DJanke@atb-potsdam.de, tamon@atb-potsdam.de

ABSTRACT

The air exchange rate is an important parameter in order to evaluate the gas emission of naturally ventilated barns. At the same time, understanding the flow inside such barns helps to evaluate the comfort of the animals inside. In this context, the local air exchange rate in sub volumes of the barn (i.e. individual animal occupied zones) is far more interesting than the total air exchange rate. Yet even the total air exchange rate is difficult to assess mainly because of fluctuating influence stimuli such as wind (speed and direction), temperature, barn geometry etc.

One objective of the BELUVA project, financed by the German Research Foundation, is to address those influences and derive a parametric function for local air exchange rates. The function will further permit to answer questions associated with precision livestock farming. For example, for a given length/width ratio of a barn and a given inflow speed and angle, in which animal occupied zones a supporting mechanical ventilation must be switch on.

The present study has been carried out in order to evaluate the impact of incident wind angle and barn's length/width ratio on the local air exchange rate in animal occupied zones of barns. Beforehand the numerical model has been validated with measurements done inside a boundary layer wind tunnel with a down sized 1/100 barn. Three different incident wind angles (0°, 45° and 90°) and three different ratios of barn's length (L) /barn's width (W) (L/W=2,3,4) have been considered.

The results of this simplified model show that, while the barn's overall air exchange rate is independent of the length to width ratio, the ones for animal occupied zones inside the barn are not. The local air exchange rate depends strongly on the position inside the barn and the velocity incident angle.

A model extension towards a full-scale building with surroundings and including the effects of animals as obstacles and heat sources is on-going in order to further increase the accuracy of the predicted local air exchange rates.

Keywords*:* air exchange rate, computational fluid dynamics (cfd) simulation, model validation, animal occupied zone***.***

1. INTRODUCTION

Recently applying computational fluid dynamics (cfd) simulations in order to study and analyze barn flow has become a common trend. Many numerical and experimental investigations on the effect of barn's geometrical design on the flow in and around naturally ventilated barns (NVB) have been done. For example, Saha et al. (2014) analyzed numerically the influence of different opening combinations on the flow inside the NVB. The author found out that the air exchange rate (AER) for the different configurations can change from 1.75 to 3 when compared to the standard configuration. Here however, the individual animal occupied zones (AOZ) were not been taken into account and the wind direction has been unchanged. Similar recent studies were done by Qianying (2017) and Gebremedhin (2004).

Another interesting, yet unexplored geometrical parameter is the length/width ratio of the barn. Indeed in Germany, barns have a typical geometry consisting of two lines of animal zones facing each other and separated by a way in the middle, in which the feed is provided ad libitum. Depending on the number of cows, those lines can get relatively long, i.e. there are high L/W ratios. In accordance with the German Federal ministry of food and agriculture (BMEL), barns are classed per number of animals and there is a recommendation of the place needed for one cow depending on body size. A survey conducted by the same ministry from 2007 to 2016 shows that even if the number of handled cattle in barns has remained relatively constant, the number of barns handling at least 100 cattle and more has increased from 22.4 % (corresponding to 63.2 % of the cattle in Germany in 2007) to 31.3 % (corresponding to 75.2 % of the cattle in Germany in 2016). The barns handling more than 200 cattle have doubled. One can conclude that in recent years, barns' size has been growing. Therefore for this study, we choose L/W = 2, 3 and 4 as representative values and a good compromise to keep the computational time reasonable.

2. VALIDATION

2.1 Atmospheric boundary layer

A preliminary study in a completely empty domain was conducted to make sure that the atmospheric boundary layer stays unchanged along the domain. Another goal was to find out the roughness corresponding to the experimental setup, to be able to implement it in the simulation. According to this roughness height, the corresponding wall functions to calculate the velocity at the wall are used in Ansys Fluent. The roughness found for the simulations is k_S=0.0065 mm. The atmospheric boundary layer profile follows the corresponding equation given in Durbin et al., 2001 and Blocken et al., 2007:

$$U(y) = U_{ref} \times \frac{\ln\left(\frac{y}{y_0}\right)}{\ln\left(\frac{y_{ref}}{y_0}\right)}$$

In Ansys Fluent the roughness is defined as:

$$k_s = \frac{9.793\, y_0}{C_s}$$

Where *U(y)* is the wind velocity at the height *y*, U_{ref} a reference velocity at a reference height y_{ref} and C_S a roughness constant with a standard value of 0.5 (Blocken et al., 2007).

2.2 Model set up and grid convergence study

The barn was placed in the middle of an empty domain. *L* is the characteristic length, *H* is the characteristic height of the barn, 4 *L* is the distance from barn to domain's inlet, 6 *L* is the distance to the domain's outlet, 10 *H* to the top and 5 *H* to the sides. A mesh refinement box around the barn was also included according to Fluent recommendations (Lanfrit, 2005).

A grid convergence study was conducted in order to find the mesh that allows a reduced computing time while ensuring the required precision. The domain mesh was a combination of a structured (quadrilateral) and an unstructured (tetrahedral) mesh. The mesh was finer within the refinement box with the smallest cells and growing gradually towards the domain boundaries with the biggest cells. The finest mesh with 1 mm cell size for the barn was the reference mesh. The grid convergence study was conducted in 2.5 *D*, which means that the domain has been cut in the middle in the flow direction with 1 mm width. In doing so, the cells numbers and thus the computing times are considerably reduced while keeping the main regions of interest sufficiently resolved. This provides fast simulations (10 to 30 min) and accurate results of the study. The velocity profiles in the barn's middle from meshes with bigger cell size are compared with the reference mesh (1 mm). The resulting discrepancies are shown in Fig. 1. The discrepancies are relatively small (1 %) and approximately constant up to the cell size of 4 mm and then increase. Therefore a 4 mm cell size was chosen for the study. The cell number for the corresponding 3D case is around 6 million cells.

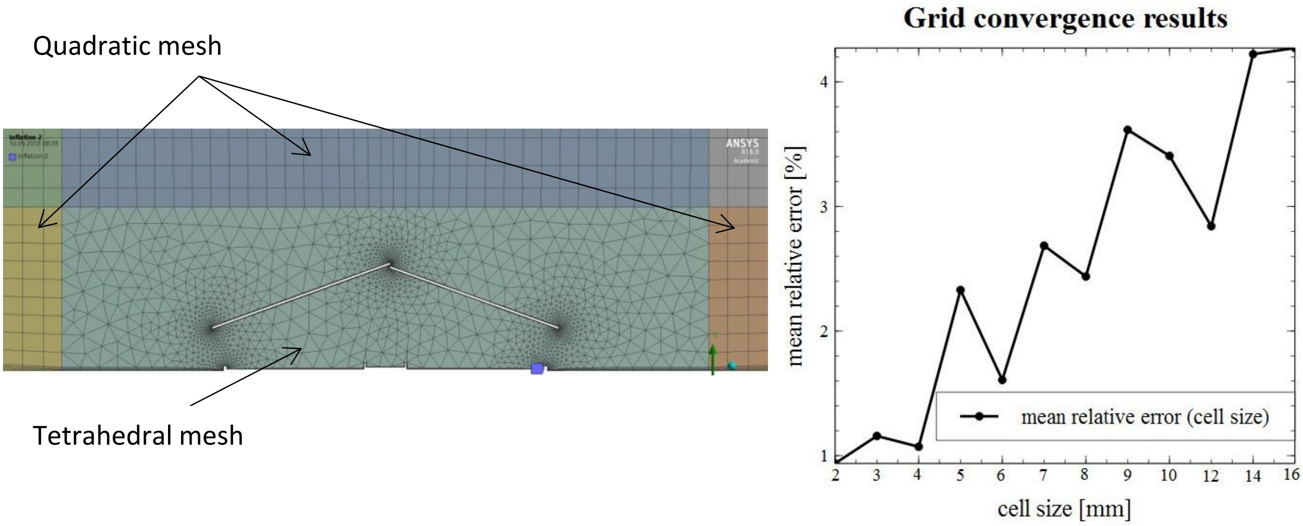

Figure 1. Left: Hybrid mesh 2.5D, Right: Grid convergence results

2.3 Model validation results

In the Leibniz Institute for Agricultural Engineering and Bioeconomy (ATB) wind tunnel measurements were carried out in order to determine the velocity profiles in and around a barn (see fig. 2). The barn was a 1:100 downscaled model from a barn situated in Dummersdorf (north Germany). Laser Doppler Anemometer measurements with a measurement uncertainty of 0.2 % were used.

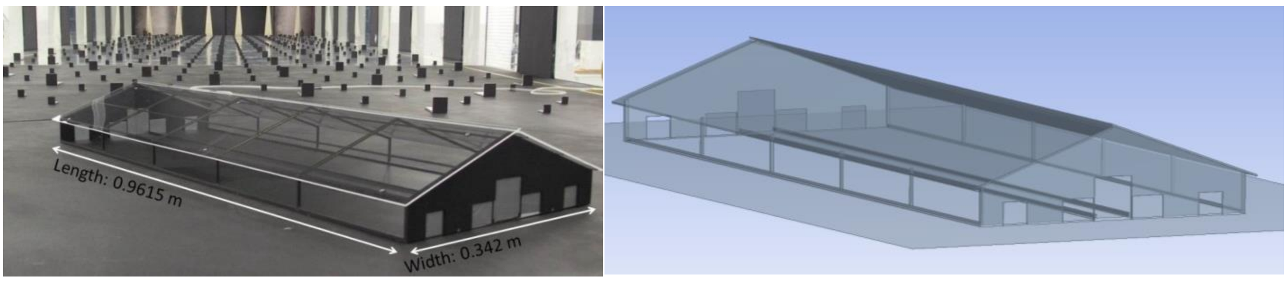

Figure 2. Left: 1:100 scale barn in wind tunnel, right: CAD model of scale barn

The experiment was used to validate the numerical model. The modeled barn geometry has been tested with the two mesh types: (1) a mesh with tetrahedral cells only and (2) a mesh with a combination of a structured (quadrilateral) and an unstructured (tetrahedral) mesh. Fig. 3 illustrates the comparisons of the velocity profiles in front of and behind the barn. The velocity profiles from the numerical simulation are in good agreement with the wind tunnel data.

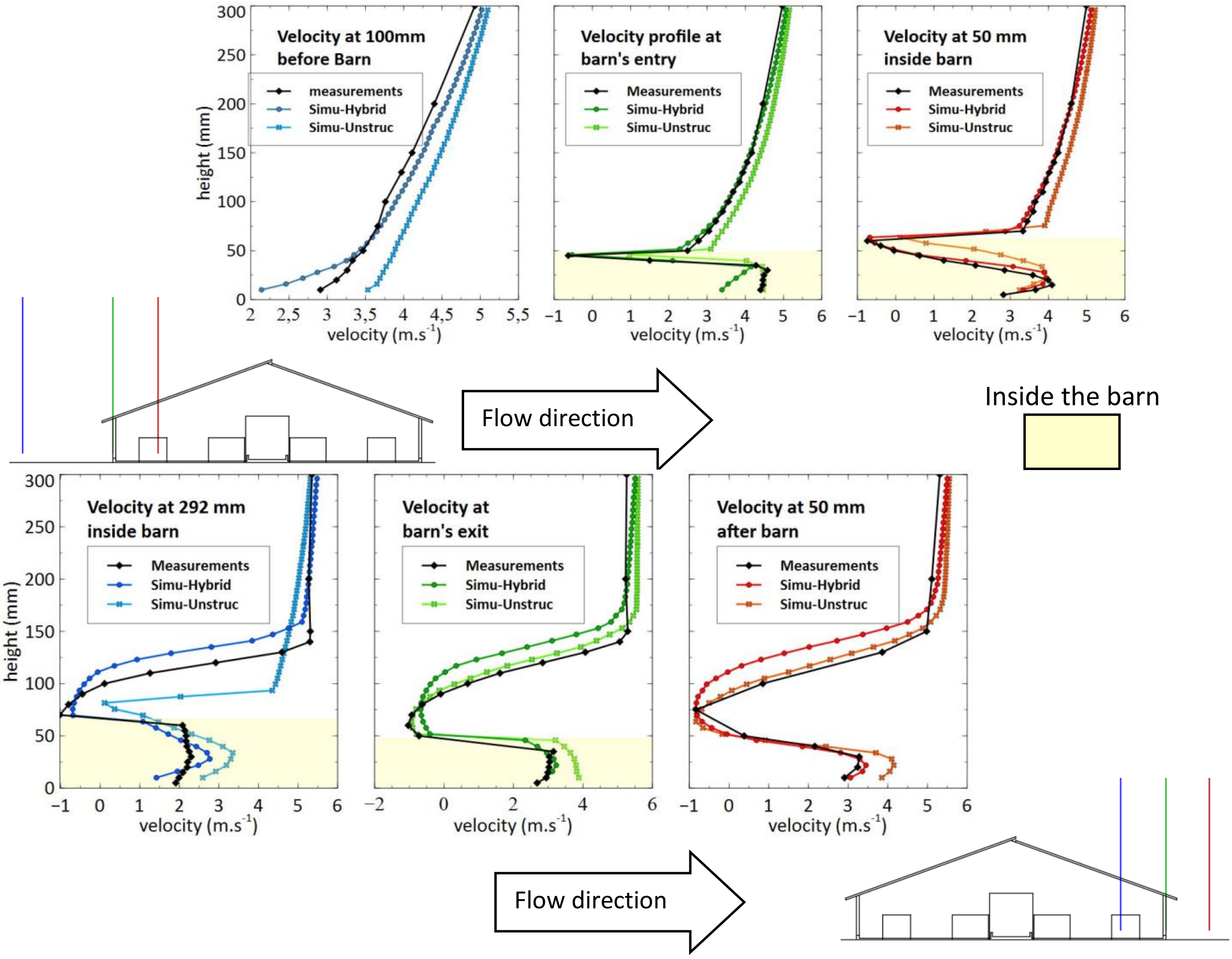

Figure 3. Model validation by comparing the vertical velocity profiles

3. RESULTS AND DISCUSSION

After the numerical model was validated, a series of simulations were carried out in order to understand the influence of barn design and the incident velocity angle degree. Since the validation was successful in scaled dimension, it was decided to keep the same scale (wind tunnel scale) for this investigation. The barn width/length ratio varied from 2 to 4 and the chosen incident wind directions were 0°, 45° and 90° degrees. Since the barn's geometry and AOZ placement are symmetric in the *x* and *y* directions, those directions are sufficient to represent incident flow from all directions. In addition, the velocity magnitude of the wind entering the barn was varied as well by 1, 3 and 5 m s^{-1}. A particular attention was paid at the AOZs inside the barn (nominated X_aZ_b, with a=1,2 and b=1..L/W). These zones are important, since their air exchange rate (denoted AER_{AOZ} in the following) gives the information of how much fresh air the animals are receiving and if this amount is sufficient. Fig. 4 shows the AER magnitude as color-coded maps for 0°, 45° and 90° incident velocity angle (from left to right) for an incident velocity of magnitude 5 m s^{-1}. One can notice that there is a distinct pattern for each incident velocity angle.

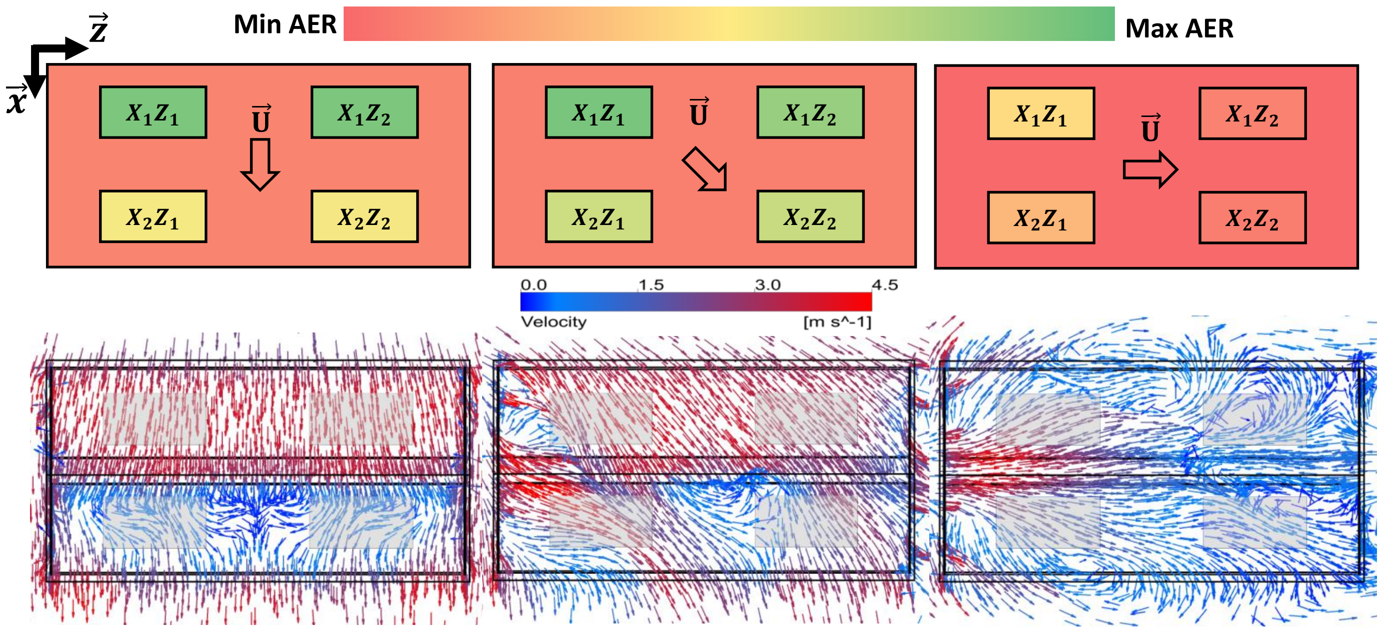

Figure 4. Up: AER of the whole barn *L/W*=2 and the AOZs for different incident velocity angles (from left to right: 0°, 45°, 90°), down: corresponding velocity vector field at the middle of AOZ height; velocity magnitude 5 m/s.

For the 0° angle case, the AER_{AOZ} of X_2Z_1 and X_2Z_2 are around half the AER_{AOZ} of X_1Z_1 and X_1Z_2. The AER_{AOZ} are more uniform for the 45° angle case. In the case of 90°, where the air enters the barn mainly through the gates of the side wall, the AER are the smallest of the three incident angles. The same patterns can be observed for the other velocity magnitude 1 m s^{-1} and 3 m s^{-1}.

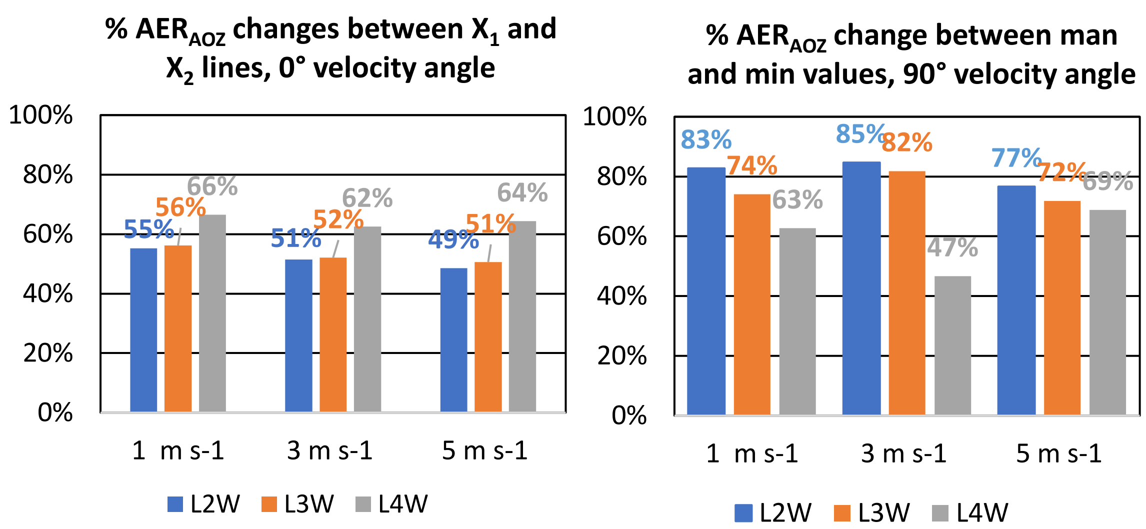

Figure 5. Left: Percentage of $(AER_{X1}-AER_{X2})/AER_{X1}$, 0° incident angle; Right: Percentage of AER_{AOZ} (max-min)/max, 90° incident angle; for all *L/W*.

Fig. 5 shows the quantitative impact of the velocity magnitude on the AER_{AOZ} for 0° (i.e. cross flow) case and the 90° (i.e. side flow) case. The left graphic compares in percentage the difference between the average AER_{AOZ} of the first line (X_2) and the second line (X_2) for all L/W ratios for the 0° case. With increasing velocity a slight decreasing trend is observed in the AER_{AOZ} (except for the case *L/W*=4 with 5 m s^{-1}). In addition, for all studied velocities, there is a more significant decrease of the AER_{AOZ} of the second line X_2 relative to the first line when *L/W*=4 (around 35 % the AER_{AOZ} of the first line X_1) compared to *L/W*=2 and 3 (around 50 % the AER_{AOZ} of the first line). The right graphic of Fig. 5 shows quantitatively the relative difference height of variation between the extreme values (max and min) of AER_{AOZ} for the 90° incident angle. The minimum AER_{AOZ} is typically more than 1/3 of the maximum AER_{AOZ}. For longer barns (bigger *L/W*), the difference between max and min AER_{AOZ} is becoming smaller while an opposite trend can be observed for 0° case.

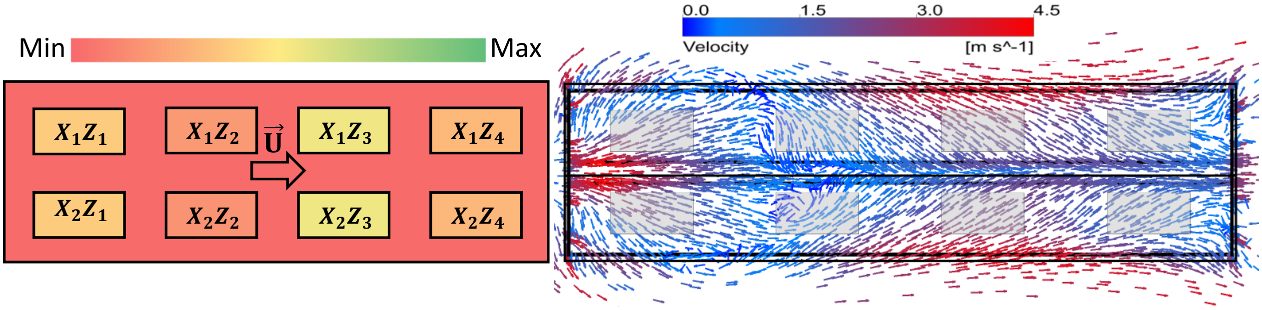

Figure 6. Left: Barn AER and AER_{AOZ}, L/W=4, 90° incident angle, 5 m s^{-1}; Right: corresponding velocity vector field.

Another interesting pattern can be seen for 90° incident angle in Figure 6. The AER of the AOZs are almost symmetric with respect to the z direction and are alternating between high and low values from one AOZ to the next one.

4. Conclusions

This study provides valuable qualitative and quantitative information about the air flow in a naturally ventilated barn. For incident wind in prevailing wind direction (0°) and perpendicular to this direction (90°) the lowest value among the air exchange rates of the individual animal occupied zones, min(AER_{AOZ}), was at least one third of the maximum value, max(AER_{AOZ}). For a 45° incident wind angle the differences between the individual AER_{AOZ} were the smallest. For the 90° incident wind angle the lowest local air exchange rates were observed. Each incident wind angle produces a particular pattern inside the barn, with a tendency to higher values at the windward side of the building. For 90° an oscillation pattern was observed.

Future work will take into account the convection and gas flow in a real sized barn in the pursuance of a better comprehension of AER dependency.

References

Saha, C.K. (2014) 'Assessing effects of different opening combinations on airflow pattern and air exchange rate of a naturally ventilated dairy building', Proceedings International Conference of Agricultural Engineering, Zurich, 06-10.07.2014.

Qianying, Y. (2017) 'Wind Tunnel Investigations of Sidewall Opening Effects on Indoor Airflows of a Cross-Ventilated Dairy Building', Energy & Buildings. doi: 10.1016/j.enbuild.2018.07.026.

Gebremedhin, K.G. (2004) 'Simulation of flow field of a ventilated and occupied animal space with different inlet and outlet conditions', Journal of Thermal Biology. doi: 10.1016/j.jtherbio.2004.10.001.

Durbin, P.A. (2001) 'Statistical Theory and Modelling for Turbulent Flows', John Wiley &Sons. ISBN 0-471-49744-4.

Blocken, B. (2017) 'CFD simulation of the atmospheric boundary layer: wall function problems', Atmospheric Environment. doi: 10.1016/j.atmosenv.2006.08.019.

Lanfrit, M. (2005) 'Best practice guidelines for handling Automotive External Aerodynamics with FLUENT'.

Statisches Jahrbuch über Ernährung, Landwirtschaft und Forsten der Bundesrepublik Deutschland (2017).